Engineering 7 (2021) 50–62

Contents lists available at ScienceDirect

Engineering

journal homepage: www.elsevier.com/locate/eng

Research
Frontiers of Chemical Engineering—Review

Membrane Crystallization for Process Intensification and Control: A Review

Xiaobin Jiang *, Yushan Shao, Lei Sheng, Peiyu Li, Gaohong He *

State Key Laboratory of Fine Chemicals, School of Chemical Engineering, Dalian University of Technology, Dalian 116024, China

ARTICLE INFO

Article history:
Received 12 March 2020
Revised 28 May 2020
Accepted 19 June 2020
Available online 8 December 2020

Keywords:
Membrane crystallization
Nucleation
Process control
Process intensification

ABSTRACT

Crystallization is a fundamental separation technology used for the production of particulate solids. Accurate nucleation and growth process control are vitally important but difficult. A novel controlling technology that can simultaneously intensify the overall crystallization process remains a significant challenge. Membrane crystallization (MCr), which has progressed significantly in recent years, is a hybrid technology platform with great potential to address this goal. This review illustrates the basic concepts of MCr and its promising applications for crystallization control and process intensification, including a state-of-the-art review of key MCr-utilized membrane materials, process control mechanisms, and optimization strategies based on diverse hybrid membranes and crystallization processes. Finally, efforts to promote MCr technology to industrial use, unexplored issues, and open questions to be addressed are outlined.

1. Introduction

Crystallization is a classic and fundamental separation technology in both chemical process engineering and product engineering, and it has achieved wide application in fields such as chemical engineering, pharmaceutical sciences, biochemical engineering, and food engineering [1–6]. The promotion of nucleation and control of the competition between nucleation and growth are core concerns because they affect both separation efficiency and product purity [7–11].

Membrane crystallization (MCr), a hybrid membrane crystallization process where a solution becomes supersaturated to simultaneously achieve solution separation and component solidification, has made great progress over the last decade [12–16]. As a highly tunable and environmentally benign technology, one of the most inspiring applications of MCr is using the membrane to serve as a heterogeneous nucleation interface to trigger the nucleation process [17–20], which opens a new research direction for MCr-customized membrane materials. With the unique advantages of membrane technology and enhanced energy utilization efficiency [13,15,21–23], MCr can manufacture the desired solid particles and ultrapure solvent with relatively low energy input [24–26].

In addition, as the customized MCr materials can result in a device with high packing density, the membrane module and related hybrid process can achieve a higher manufacturing capacity and intensified separation process than conventional crystallization can achieve [27–30]. The total mass transfer (or heat transfer) coefficient of the membrane module can guarantee sufficient supersaturation for diverse crystallization modes (e.g., evaporative crystallization, antisolvent crystallization, and cooling crystallization), which is also an attractive topic for novel process engineering development. Meanwhile, intensification of the crystallization process is also directed toward substantially smaller, cleaner, and more energy-efficient technology and devices [31–33].

All the above features make MCr research, including specific materials fabrication, device development, and process design, vibrant and challenging. In this review, we present an overview of the novel contribution of MCr to accurate process control and intensification, then outline the remaining challenges and imperative issues yet to be solved.

2. Principles of MCr and typical membranes

2.1. Principles of MCr

MCr is not limited to membrane separation technology followed by downstream crystallization. Basic and applied research

* Corresponding authors.
E-mail addresses: xbjiang@dlut.edu.cn (X. Jiang), hgaohong@dlut.edu.cn (G. He).

https://doi.org/10.1016/j.eng.2020.06.024

developments have quickly expanded MCr to cover membrane-assisted industrial crystallization, *in situ* nucleation and growth on membrane interfaces, and novel solid formation involving a membrane. Currently, diverse crystallization modes (cooling, evaporative, antisolvent crystallization, and reactive modes) can be coupled with membrane separation technology for diverse MCr operations. Among these, membrane distillation with crystallization (MDCr) is considered an emerging hybrid approach that integrates membrane distillation and traditional crystallization processes. The most crucial feature of MDCr is membranes with finely controlled performance [34,35].

It is commonly accepted that solvents recovery via an effective distillation separation process is easily achievable through a membrane interface. Accordingly, in the MDCr process, the hydrophobic microporous membranes are operated as an interface for vapor and liquid separation, which allows only solvent vapor to pass through the membrane pores while preventing the passage of liquid solvent [36]. The gradient vapor pressure results in evaporation of a volatile component from the feed side and condensation at the permeate side. One kind of classic membrane crystallizer (Fig. 1 [37]) generates supersaturation and finally promotes the crystallization process via distillation of the solvent (antisolvent) from the feed solution to the permeate side [38]. Therefore, the membrane in MCr does not serve as screening barrier for components transport, but as a support layer for generating and maintaining a controlled supersaturated environment for nucleation and crystal growth.

It should be also noted that during MCr operation there is a certain mass transfer boundary layer in the feed side near the membrane interface where the nonvolatile component has relatively higher concentration than in the bulk solution owing to the concentration polarization effect. The porous structure on the membrane surface can provide a heterogeneous interface in which solute molecules can be embedded, resulting in reinforced supersaturation [38]. When the solution concentration reaches a supersaturated state in the boundary layer, interaction between the membrane surface and the solute molecules facilitates proper crystal nucleation. After a certain extent of growth, the crystals detach from the interface and supply crystal seeds to promote uniform crystallization in the bulk solution [39]. Accordingly, the membrane surface acts as a physical substrate able to reduce the free energy barrier and promote heterogeneous nucleation [37,40].

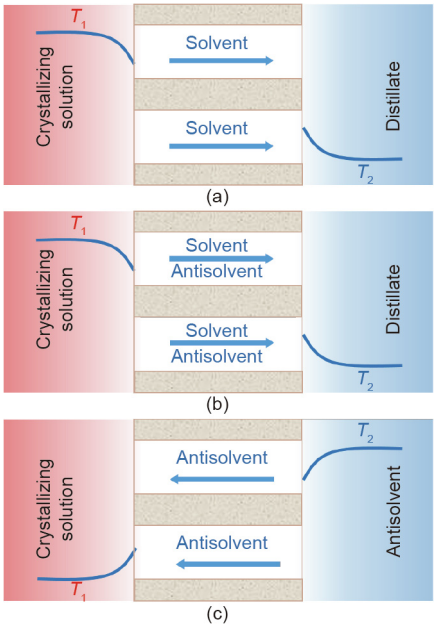

Fig. 1. Schematic of antisolvent crystallization principles: (a) solvent removal MCr ($T_1 > T_2$), (b) solvent/antisolvent demixing MCr ($T_1 > T_2$), and (c) antisolvent addition MCr ($T_1 < T_2$). T_1: temperature of crystallization; T_2: temperature of distillate or antisolvent. Reproduced from Ref. [37] with permission of Elsevier Ltd., ©2012.

2.2. Polymeric and other membranes for MCr

Porous polymeric membranes have been widely investigated in recent decades for a variety of MCr applications, such as wastewater treatment [41] and solid product separation, as well as ultrapure solvent recovery [24–26,42,43]. The most typical membranes used in existing MCr processes are those fabricated from organic polymeric materials containing polypropylene (PP), polyvinylidene fluoride (PVDF), polytetrafluoroethylene (PTFE), and polyethersulfone (PES), which are common porous membranes with pores ranging from the subnano- to micron-scale [44–46].

PES membranes have been used for solvent removal because they provide a high alternative surface area and thus achieve the necessary operability, controllability, and enhanced micromixing [29]. In recent years, PES membranes (Fig. 2) have been used for erythritol purification via an antisolvent crystallization process [29]. The cross section of the hydrophilic PES hollow fiber membranes used in this process exhibits an asymmetric structure with a very thin layer and possesses a relatively high porosity of 58%. Benefitting from these nanoscale pores, a membrane module was successfully introduced to realize transfer and microscale mixing between the crystallization solution and organic antisolvent, thereby reducing the local supersaturated environment. As seen in Fig. 3, the organic antisolvent permeating rate can be accurately controlled by the flow velocity of the shell side and tube side depending on the structure of the PES membrane, hence guaranteeing an accurate antisolvent gradient and degree of supersaturation [29].

Owing to its high permeate flux and excellent mechanical features, a PVDF membrane with microporous structure and hydrophobicity has been widely used in MCr for mineral recovery and hypersaline water desalination [47,48]. Microporous PVDF can be easily produced by phase inversion and other simple methods because of its easy processability. In addition, PVDF exhibits superior thermodynamic and chemical compatibility with other polymers and can be further modified with inorganic materials to obtain desired functions. Thermal stability has been considered the most crucial parameter in a variety of applications. Generally, the abundant fluorine atoms and carbon (C)–fluoride (F) bonds in PVDF ensure the high stability of the materials, and they possess excellent performance under high-temperature operations

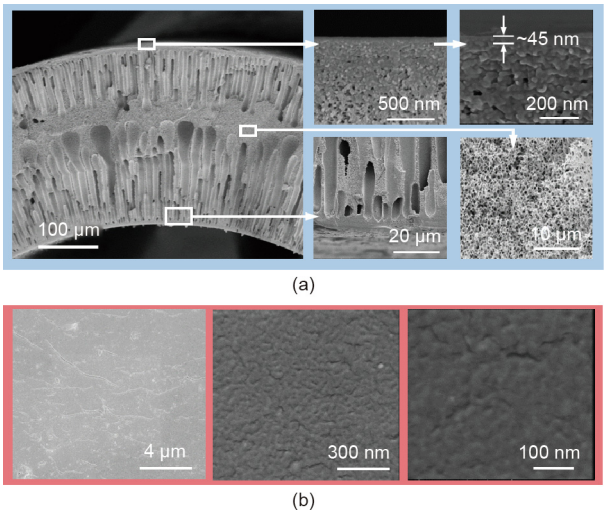

Fig. 2. PES membrane morphologies of (a) cross section and (b) membrane surface. Reproduced from Ref. [29] with permission of Elsevier Ltd., ©2019.

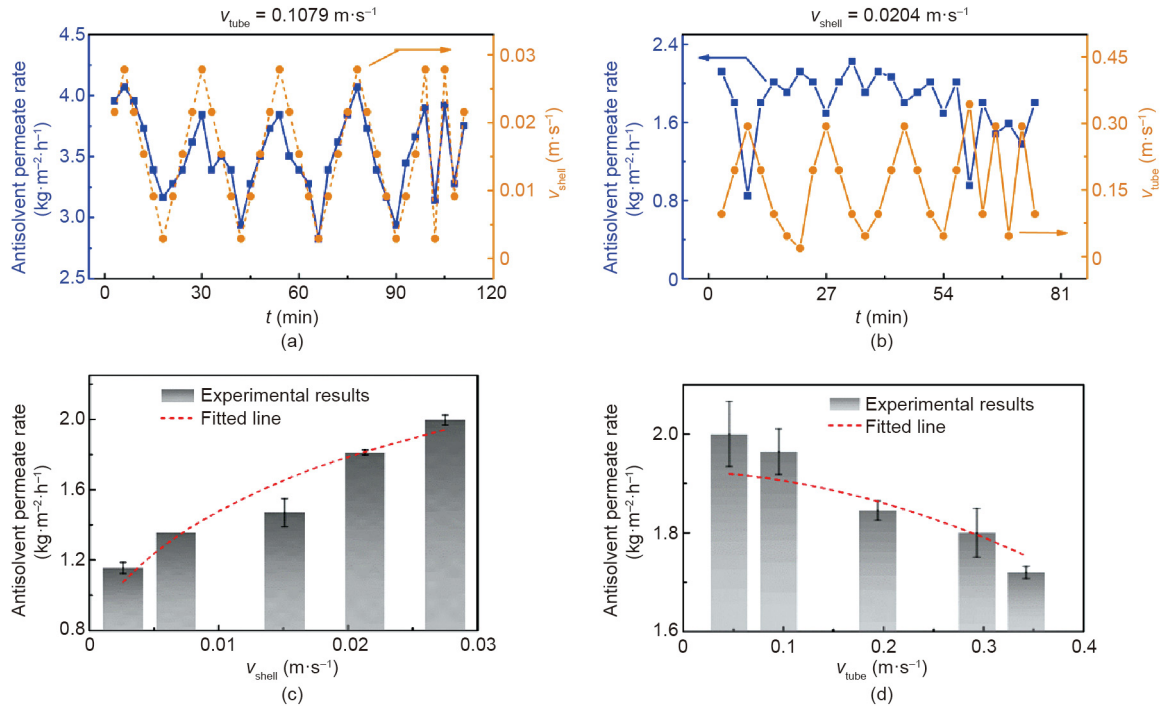

Fig. 3. Antisolvent permeate rate under different velocities of (a) shell side flow velocity (v_{shell}) and (b) tube side flow velocity (v_{tube}); comparison of antisolvent permeate rates of various (c) v_{shell} and (d) v_{tube}. Reproduced from Ref. [29] with permission of Elsevier Ltd., ©2019.

[13,49]. As a result of its distinct chemical stability, PVDF membranes can be particularly applied to acid gas absorption and wastewater treatment because it can resist a large number of harsh chemicals, including inorganic acids, oxidants, and halogens, as well as aromatic, chlorinated, and aliphatic solvents [50,51].

To date, a large number of investigators have reported the application of PVDF membranes in membrane contactors for salt crystallization and high-salinity wastewater treatment. Feng et al. [48] prepared a synthetic review of PVDF membranes applied to membrane-based processes such as gas separation and membrane distillation for the removal of volatile organic compounds. Early investigations indicated the effect of the surface structure of the PVDF hollow fiber membranes (Fig. 4 [51]) on their performance when used for high-saline water treatment in direct contact membrane distillation (DCMD). The results showed a stable permeation flux and lesser membrane permeability reduction for the dual-layer (DL)-PVDF–polyacrylonitrile (PAN) membrane as a result of its optimized pore structure along with its hybrid morphology of a macropore-free cellular structure and dense structure (Fig. 5) [51].

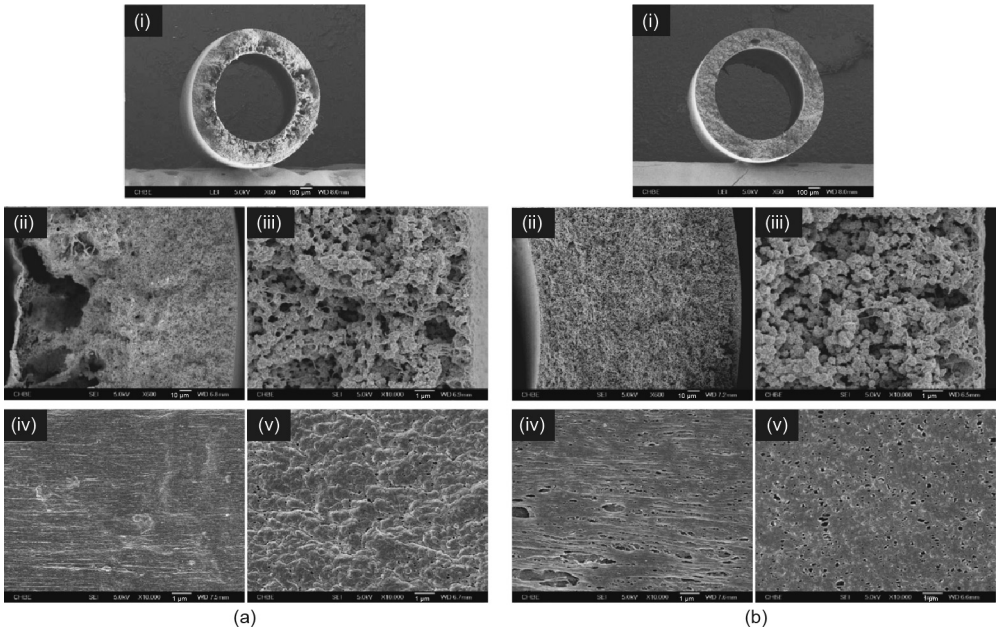

Fig. 4. Scanning electron microscope (SEM) images of (a) DL-PVDF–PAN membrane and (b) DL-PVDF membrane: (i) cross section, (ii) magnifying cross section, (iii) outer layer, (iv) inner surface, and (v) outer surface. DL: dual-layer. Reproduced from Ref. [51] with permission of Elsevier Ltd., ©2003.

Anisi et al. [52] tested optimal conditions for membrane distillation (MD) and batch seed crystallization processes to evaluate the feasibility of a PVDF membrane unit to generate supersaturation and determine a model of the heat and mass transfer mechanism. Jiang et al. [22] investigated the influence of membrane properties and the type of membrane module on crystal nucleation and found that membrane porosity plays a significant role in reducing the nucleation barrier for membrane-assisted cooling crystallization. Further investigation by Choi et al. [53] revealed crystal growth and formation during a fractional-submerged MDCr process equipped with PVDF hollow fiber membranes for brine treatment, which indicated the diversity of the initial crystallization point on the reactor and the membrane surface at different temperatures.

PP membranes, which have high porosity and hydrophobicity, also have a wide range of applications in MCr [23,26,30]. Investigations have indicated PP hollow fiber membranes with desired porosity and structures were preferable materials for the proposed MCr until now. In addition, by comparing different MCr performances in vacuum and direct contact configurations, many studies have shown that PP membranes can be applied to vacuum membrane distillation (VMD) both in single- and mixed-salt solutions for water and salt recovery [54,55].

In addition to aforementioned organic materials, composite membranes are crucial not only for desalination but also for biomacromolecule and protein crystallization processes [37,56–58]. Wang et al. [59] developed a new MCr membrane for continuous protein crystallization which can ensure high selectivity of the crystal morphologies with robust performance. The fabricated *N*-isopropylacrylamide (NIPAM)–polyethylene glycol diacrylate (PEGDA) hydrogel composite membranes (HCMs) realized stable crystal productivity, and crystals with the desired hexagonal cube and brand-new flower morphologies were efficiently generated with high morphology selectivity, which can simultaneously intensify the crystallization process and improve production efficiency via continuous ion concentration control (Fig. 6 [59]).

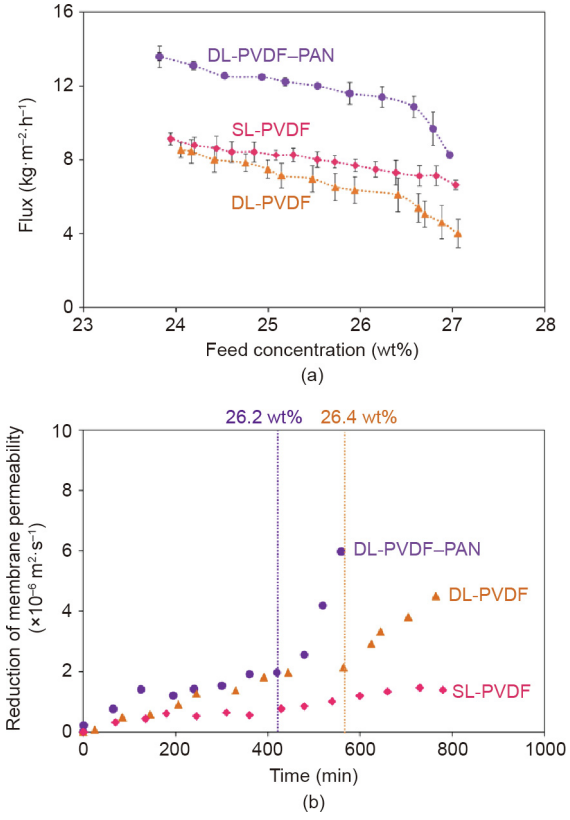

Fig. 5. (a) Permeate flux and (b) membrane permeability reduction for different hollow fiber membranes. SL: single-layer. Reproduced from Ref. [51] with permission of Elsevier Ltd., ©2003.

Thus, the list of membranes appropriate for MCr is growing and the potential of MCr is expanding. Besides the desired interfacial selective transfer property and stable chemical and mechanical properties, the features of nucleation induction, adjustability, and quick environmental responsiveness to the crystallization system may be the crucial requirements of MCr-utilized membranes.

3. Intensified transfer process via MCr

Generally, the aim of process intensification is safer and sustainable technological developments by the way of methods such as miniaturization, integration, and advanced mixing technology [32]. The new tendency of crystallization process intensification is accurate mass transfer regulation and uniform distribution of supersaturation under improved crystallization efficiency, which covers a broad range of transfer process intensification from the microscale (crystal cluster or nucleus) to the macroscale (crystallizer). To obtain specific crystal products with high purity, narrower crystal size distribution (CSD), and better morphology, tremendous efforts have been made to strengthen the process and improve the mixing state by using a microstructure reactor [60–62] or external fields [63–67]. A membrane module with a specific mass transfer structure (approximate two-dimensional (2D) micro-interface) has intrinsic advantages for achieving a uniform mass transfer rate and enhancing the micromixing process by controlling the distribution of the solute and crystallization solvent [26,68].

3.1. Micromixing intensification via MCr

Micromixing plays a vital role in supersaturation control for crystallization [32,69]. According to Van Gerven and Stankiewicz's [70] systematic classification of enhanced mixing, four modes of enhanced mixing (structure domain, time domain, energy domain, and function domain) can summarize the crystallization process [63,71]. The design of the micromixer can increase the mixing efficiency and reduce the mixing time by using specific structures or introducing an external energy field [72–75]. Fig. 7 shows the relationship between mixing time and the change in Reynolds number for different static mixers [76]. At a low Reynolds number, the mass transfer is almost molecular diffusion. However, the mass transfer between fluids changes to eddy diffusion under increasing turbulence, which results in a shorter mixing time. The microchannel size of the microreactor also has a large impact on the mixing time [61,77].

The dispersing function of the membrane with nano- or sub-nanochannels provides even mixing of two streams of fluid and strengthens the micromixing performance [78], which plays a vital role in controlling crystal formation. A uniform and stable supersaturated environment can be achieved by membrane interfacial dispersion for a rapid precipitation reaction to control nucleation and growth rate [79]. For example, Chen et al. [80] studied a method to produce barium sulfate nanocrystals using a membrane dispersion reactor. The average size of the crystal with spherical morphology produced by this method was adjusted to a range of 20–200 nm. Smaller barium sulfate crystals can be produced by regulating the concentration of the sodium sulfate aqueous solution and the membrane pore size. γ-Alumina nanoparticles having two peaks in the pore size distribution [81] and hexagonal ZnO

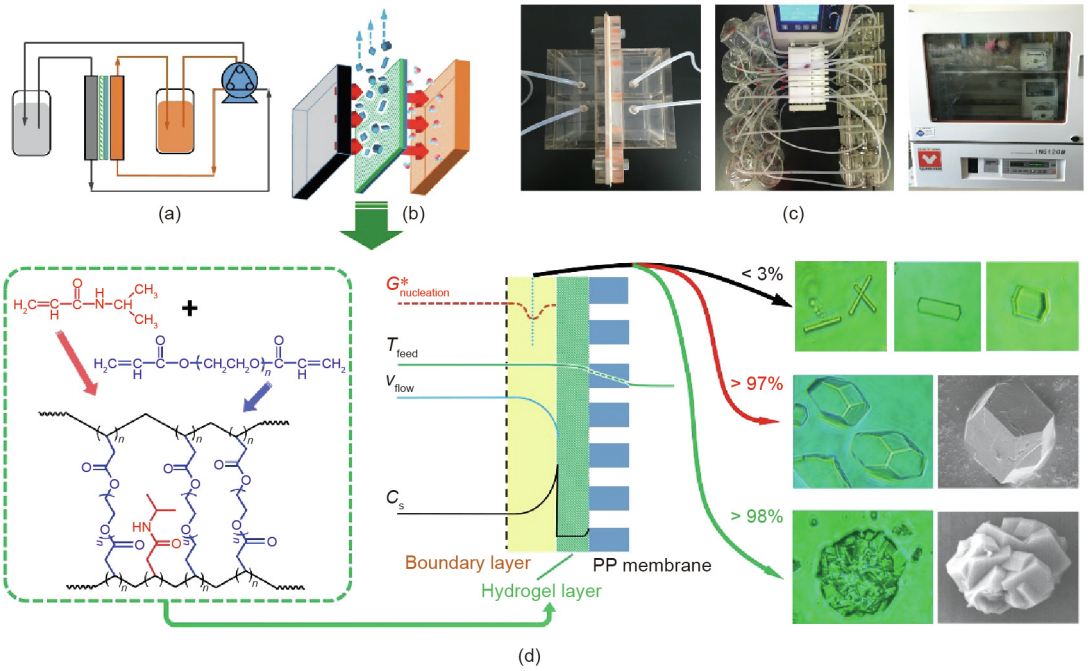

Fig. 6. (a) Experiment flow chart of the continuous MCr process; (b) schematic of membrane crystallizer; (c) actual experimental devices; (d) schematic of the dynamic interfacial HCM-assisted MCr and molecular formation principles. $G^*_{nucleation}$: the critical nucleation energy; T_{feed}: the temperature of the feed crystallization solution; v_{flow}: the velocity of the feed flow; C_s: the concentration of the crystallization component; the percentages (3%, 97%, and 98%) are the morphology selectivity. Reproduced from Ref. [59] with permission of Elsevier Ltd., ©2018.

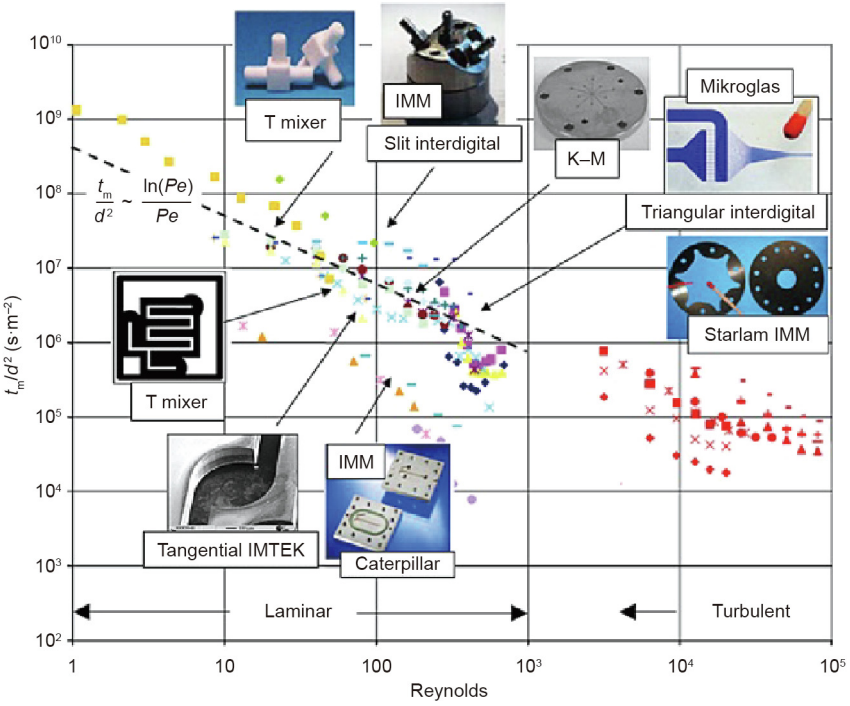

Fig. 7. Ratio of mixing time by the square of the characteristic flow dimension (t_m/d^2) with change in Reynolds number for different static mixers. t_m: mixing time; d: characteristic flow dimension; IMM: interdigital micromixer; Pe: Péclet number; IMTEK: an institute of microsystem technology in University of Freiburg (Germany); K–M: kinetic energy with molecular diffusion. Reproduced from Ref. [76] with permission of Elsevier Ltd., ©2010.

nanoparticles [82] have been successfully synthesized using a highly efficient mixed-membrane disperser.

A classic process for producing nanoparticles via MCr is shown in Fig. 8 [83]. Unlike a conventional stirring crystallizer, a membrane dispersion reactor results in size-controlled cerium dioxide (CeO_2) crystals. While the average size obtained by conventional mixing was 16.7 nm, the crystal size obtained by the membrane dispersion method was as low as 8.2 nm because of the improved mixing performance (as shown in Fig. 9) [83]. The above methods to improve mixing are all attempts to manufacture ultrafine nanoparticles and shed light on the manufacture of crystals with a specific target size for industrial applications.

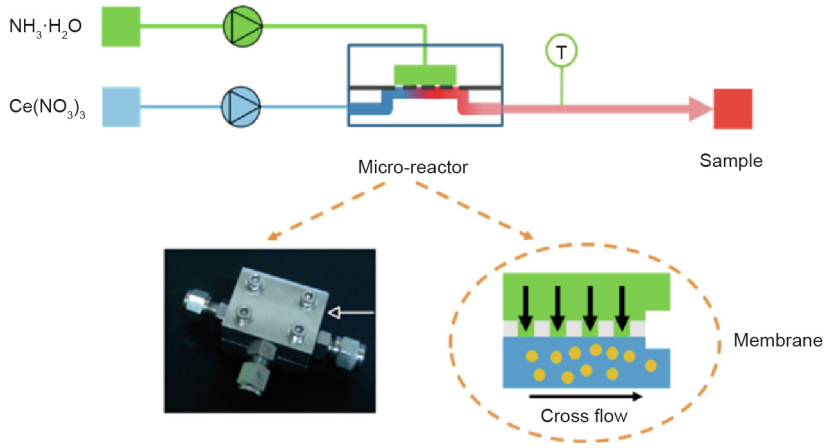

Fig. 8. Experimental setup of the membrane dispersion reactor [83]. T: the temperature meter. Reproduced from Ref. [83] with permission of Elsevier Ltd., ©2017.

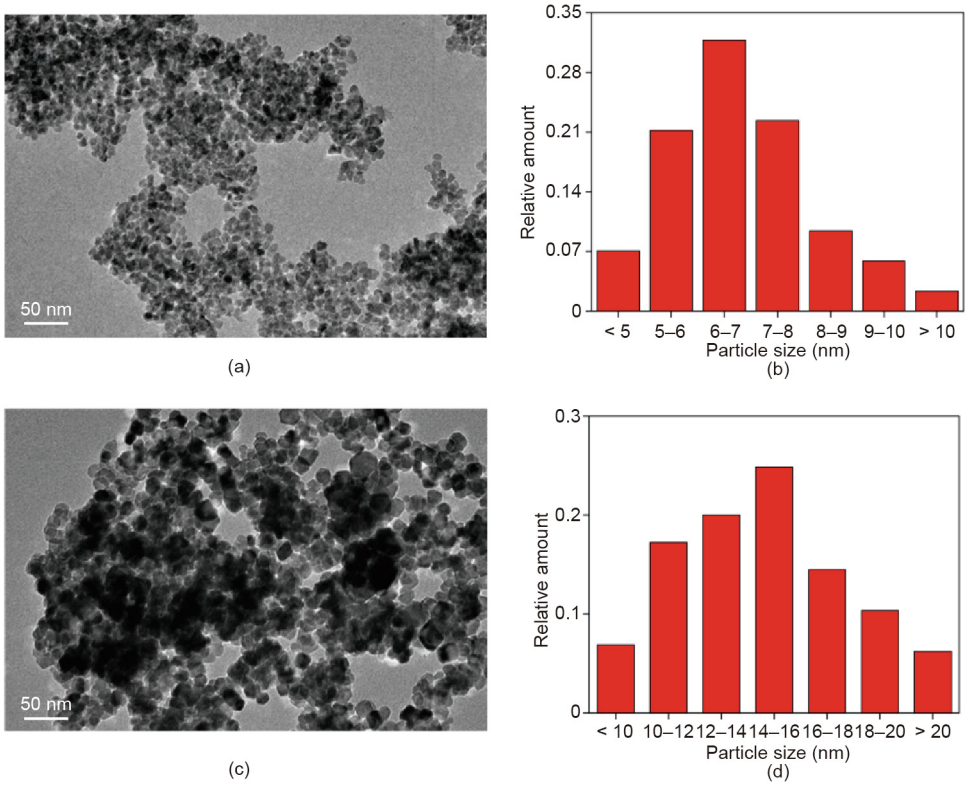

Fig. 9. Transmission electron microscopy image and particle-size distribution of CeO_2 particles obtained by (a, b) a microreactor under membrane dispersion and (c, d) stirred tank conditions. Reproduced from Ref. [83] with permission of Elsevier Ltd., ©2017.

3.2. Novel mass transfer mechanism via membrane-assisted antisolvent crystallization

A critical challenge in the crystallization process is the interfacial micromixing of the antisolvent/crystallization solution during antisolvent crystallization owing to the limited droplet surface with low interfacial mass transfer rate and high diffusion resistance. In recent years, crystal products with good morphology have been successfully obtained using equipment with porous hollow fiber membranes [84,85]. To avoid the deposition of crystal products in the hollow fiber tube and thus blocking further production, a classic feeding mode (shown in Fig. 10) is generally selected for hollow fiber porous membrane-assisted antisolvent crystallization (HFPMAAC) [25]. Chen et al. [21,44] produced polymer-coated drug nanocrystals and nanoparticles utilizing HFPMAAC. The porous membrane with micron- or submicron-channels serves as the mass transfer interface between the antisolvent and crystallization, resulting in precise mass transfer control of the antisolvent and strengthening the micromixing [86,87].

When the membrane used in membrane-assisted antisolvent crystallization (MAAC) is not porous, the mass transfer between antisolvent and crystallization follows an alternative mechanism of surface renewal rather than microdroplet mixing (Fig. 11) [29]. A precise supersaturation control mechanism was developed via permeating antisolvent on the membrane microscale interface. The new mechanism can obtain accurate supersaturation regulation in milliseconds at approximately the 2D submicron liquid layer (thickness around 50 to 200 μm), which overcomes the

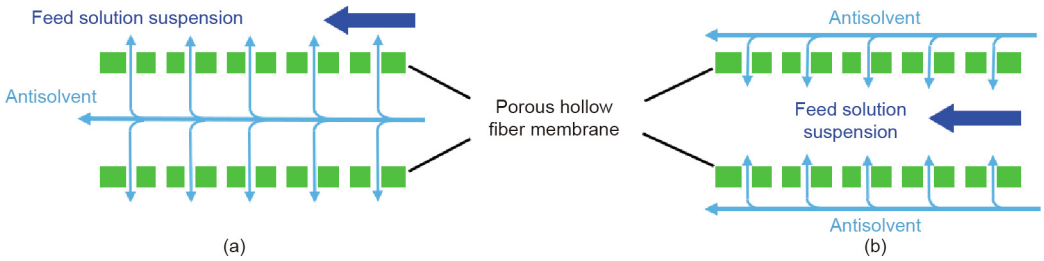

Fig. 10. Two antisolvent penetration modes of the antisolvent crystallization using a porous hollow fiber membrane: (a) antisolvent flows in the tube side and (b) antisolvent flows in the shell side. Reproduced from Ref. [25] with permission of Elsevier Ltd., ©2017.

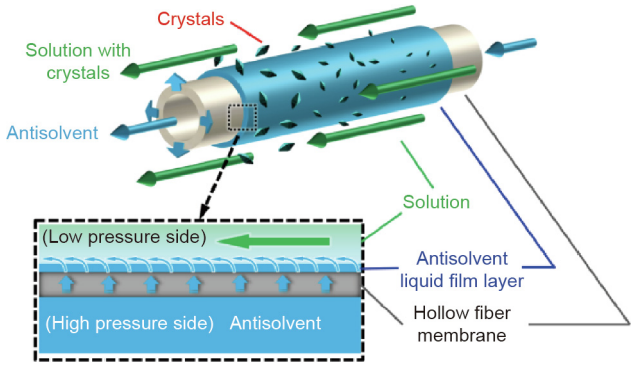

Fig. 11. Schematic diagram for MAAC process. Reproduced from Ref. [29] with permission of Elsevier Ltd., ©2019.

inhomogeneity drawback of the conventional three-dimensional (3D) macro-mass transfer that occurs in a kettle crystallizer or tubular crystallizer.

Based on the process analysis and developed model, antisolvent permeation flux can be precisely controlled by regulating the velocity in the membrane module shell side. With the MAAC advantages of low interfacial mass transfer rate and better mixing, crystals of a classic pharmaceutical product, erythritol, can be obtained with improved morphology and narrower CSD (as shown in Fig. 12 [29]). MAAC possesses more accurate control in terms of interfacial mass transfer rate (0.66 $mg \cdot cm^{-2} \cdot s^{-1}$) than conventional antisolvent crystallization owning to the membrane module with high packing density (238 $m^2 \cdot m^{-3}$). When the packing density is doubled, the interfacial mass transfer rate decreases accordingly, simultaneously improving control accuracy. The stable liquid layer formed on the membrane outer surface can effectively prevent heterogeneous nucleation attachment and enhance the antisolvent addition rate, both of which increase the manufacturing capacity of MAAC.

4. Hybrid process control and applications of MCr

The process of nucleation and growth is a core concern for determining the crystallization mechanism and realizing industrial applications. MCr is an emerging hybrid technology platform with great potential to address this concern. Unlike traditional crystallization methods, MCr can serve as a process decoupling approach: nucleate on the membrane interface (or in the membrane module) and then grow in the crystallizer (or in the membrane crystallizer system). By introducing the membrane interface, it is possible to coordinate control of the microscale force field and supersaturation environment via membrane interfacial nucleation. This is of increasing interest for complex crystallization process control and design.

4.1. Accelerating nucleation and autoseeding via MCr for process control

In the membrane-assisted crystallization process, a uniform interface is provided by the membrane, which is beneficial for precisely regulating supersaturation and mixing conditions. The membrane used in this process also functions as a heterogeneous nucleation medium, and may further increase the risk of mass transfer, efficiently reduce the fouling on the membrane surface [88,89]. Based on van der Waals friction hydrodynamic force field theory and classic nucleus kinetics, Jiang et al. [30] proposed a mathematical model to determine the nucleation and crystal growth control mechanism on the membrane interface. Three crystal modes exist on the membrane surface under certain operational conditions and particle size, including temporary adhesion, autodetachment, and perpetual adhesion (Fig. 13 [30]). The process of crystal adhesion, growth, and detachment was directly observed via real-time experiments.

The transformation from membrane scaling to nucleation autodetachment is crucial for the MCr process because the process of crystal nucleation, growth, and detachment can automatically select and screen the crystal size under specific conditions. Detached crystals transfer into the main solution as seeds for subsequent crystal growth and aging. The automatic crystal selection process can isolate the nucleation and growth process from the spatial–temporal aspect, which effectively avoids secondary nucleation in the crystallizer. Owing to the introduction of uniform seed crystals produced by the membrane, the crystal products obtained by the MCr possess have a narrower size distribution than those from non-membrane crystallization (Fig. 14 [30]).

4.2. Comprehensive solution treatment via hybrid MCr system

Because of the MCr nucleation process control and effective crystal growth adjustment, a hybrid MCr system with reverse osmosis (RO) and relevant membrane-based technology provides an improved route to comprehensive solution treatment. Macedonio et al. [90] studied an integrated membrane system for seawater desalination (Fig. 15). The plant recovery factor was greatly increased (reached 92.8%) by the introduction of MDCr. A high total-water recovery (more than 90%) was achieved by combining MDCr with the RO process, and the sodium chloride (NaCl) crystals obtained also possessed a narrow size distribution [91]. In addition, Ali et al. [92] analyzed the performance of a system that combined microfiltration (MF) with MCr for treating produced water. These studies all verified the ability to convert wastewater to freshwater and useful salt by using low-grade heat flow and MCr hybrid system.

The membrane surface is easily contaminated in the MDCr process while recovering crystals under high solution concentration conditions. Therefore, for crystals whose solubility decreases significantly with temperature, the coupling of cooling crystallization

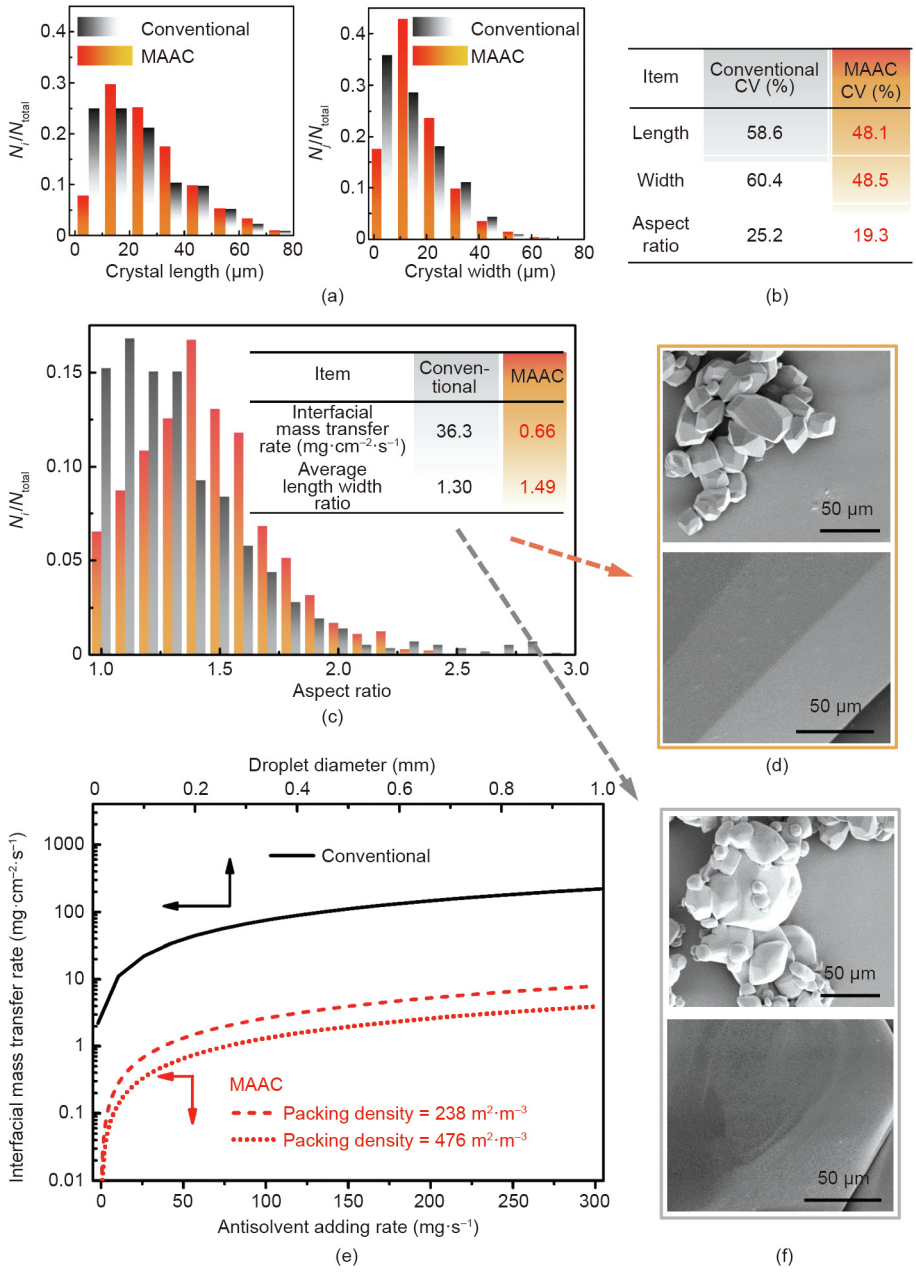

Fig. 12. Comparison of crystal properties in terms of (a) crystal length and width, (b) coefficient of variation (CV), (c) aspect ratio, (d) MAAC crystal morphology, (e) interfacial mass transfer rate, and (f) conventional crystal morphology. The crystals were obtained after 1 h of MAAC or conventional antisolvent crystallization. N_i: number of crystals with length of i μm; N_j: number of crystals with length of j μm; N_{total}: number of total crystals. Reproduced from Ref. [29] with permission of Elsevier Ltd., ©2019.

and MDCr can significantly improve crystal yield and prevent membrane fouling at the same time. For example, Wu et al. [93] found it was easy to reach high supersaturation using MD, and high-quality crystals were gained from further multistage cooling. Gryta [94] applied the MDCr process to the treatment of a concentrated NaCl solution, and with the assistance of two-stage cooling crystallization, up to 43 $kg·m^{-2}·d^{-1}$ NaCl could be obtained from the feed solution.

The energy efficiency of MDCr is an essential issue when considering diverse hybrid processes and configuration designs. There are four operation modules for MD depending on the management of the permeate side [95]: ① DCMD, where cool water is in direct contact with the membrane to absorb vapor; ② air gap membrane distillation (AGMD), which introduces an air gap near the membrane on the permeate side to reduce heat loss; ③ sweeping gas membrane distillation (SGMD), where the gas sweeps the permeate side to transfer the vapor to a condenser; and ④ VMD, where the permeate side is under vacuum or low pressure. DCMD is the most common process in laboratory-scale studies because of its simple equipment design. Compared with DCMD, the air gap in the AGMD process reduces heat loss on the membrane surface, resulting in higher energy efficiency. SGMD is appropriate for removing volatile compounds from aqueous solution [95]. Thus, this configuration has been applied in some food industries [96]. Another widely used configuration is VMD, which has a higher permeate flux compared with the other configurations as a result of its high mass transfer driving force [97]. Because the driving force of the MDCr process comes primarily from the difference in transmembrane vapor pressure, an increase in temperature can effectively improve the mass transfer efficiency by increasing the

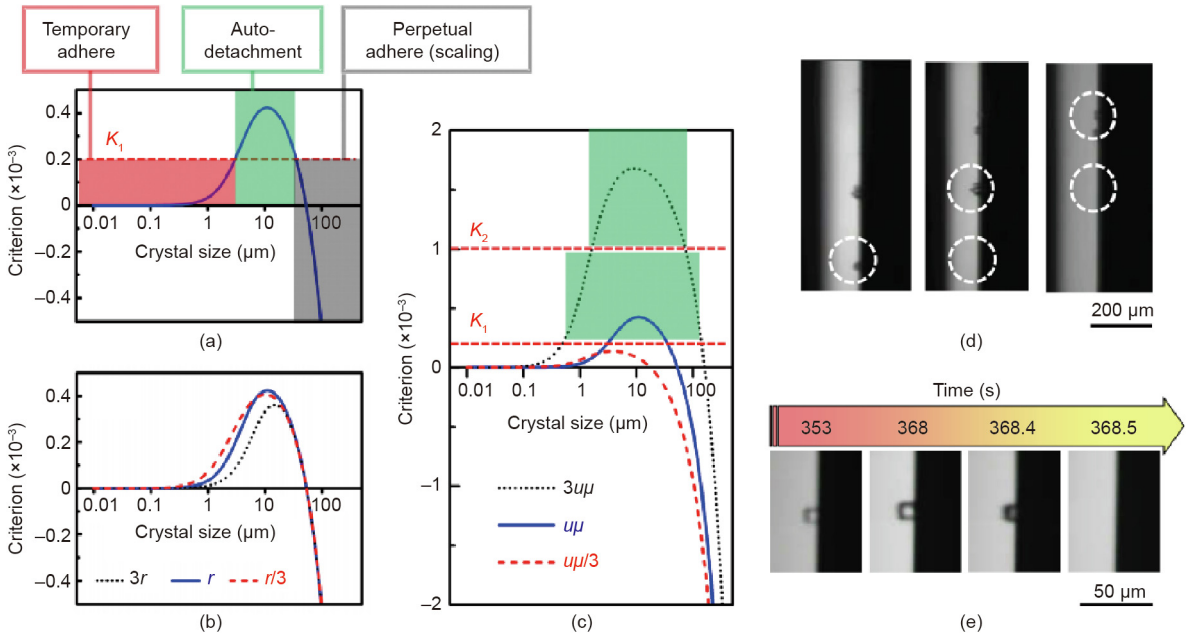

Fig. 13. (a) Simulation curve of crystal growing and detaching under (b) conditions of different membrane roughness (r) and (c) feed conditions ($u\mu$: the parameter multiplies the velocity and viscosity of solution) the parameter multiplies the velocity and viscosity of solution; (d, e) online detection of crystal detachment on the membrane surface. K_1 and K_2 are the maximum static friction coefficient under different condition. Reproduced from Ref. [30] with permission of Elsevier Ltd., ©2019.

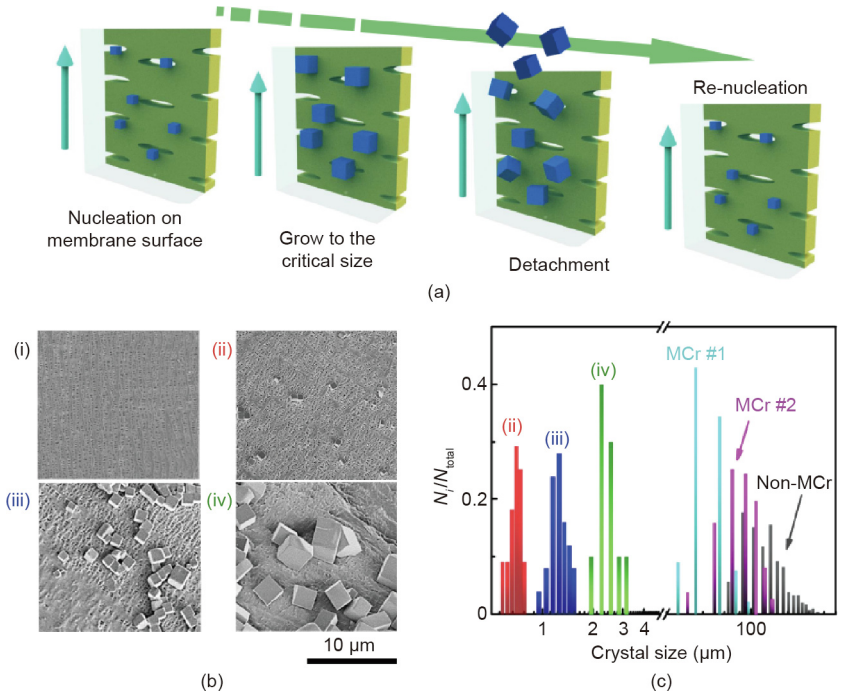

Fig. 14. (a) Mechanism diagram of nucleation, crystal growth, and detachment; (b) SEM images of (i) the original membrane surface and (ii)–(iv) the used membrane surface with uniform particle sizes after different operation times; (c) CSD comparison of conventional non-MCr, and the uniform crystals on the membrane surface and the crystal products of MCr (MCr #1: operation temperature is 60 °C; MCr #2: operation temperature is 80 °C; same feed concentration). Reproduced from Ref. [30] with permission of Elsevier Ltd., ©2019.

saturated vapor pressure on the feed side [98]. However, the effect is marginal, and simply increasing the temperature may reduce the overall thermal efficiency [99]. Furthermore, for some solutes whose solubility decreases with increasing temperature, operation at high temperatures increases the risk of membrane fouling. Therefore, it is necessary to find the optimal operating temperature appropriate for different solution systems [97].

For the MCr devices, flat-sheet and hollow fiber membrane modules are commonly applied both in laboratory-scale experiments and pilot plants [100,101]. The flat-sheet membrane module has the advantages of simple structure, convenient cleaning, and low cost, but the specific surface area and packing densities are lower than in the hollow fiber membrane module. Furthermore, Meng et al. [102] pointed out that the crystal nucleation and

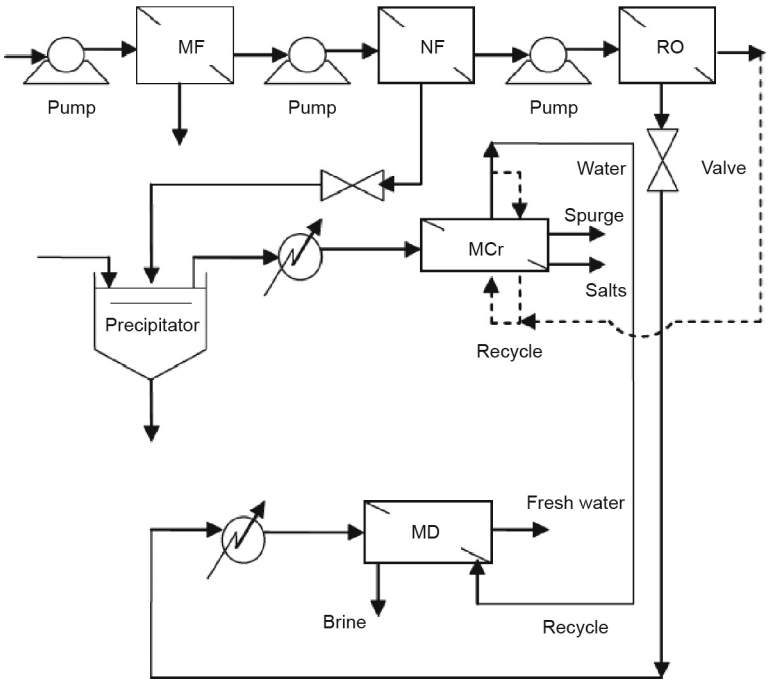

Fig. 15. Process diagram of hybrid MCr system for comprehensive saline water treatment. MF: microfiltration; NF: nanofiltration. Reproduced from Ref. [90] with permission of Elsevier Ltd., ©2007.

growth behavior of those two membrane modules were consistent, indicating both membrane modules have similar crystallization mechanisms.

In conventional MDCr operation, the feed solution is heated and pumped into the membrane module, and the concentrated solution must be reheated for the next cycle. This process produces a large amount of heat loss from the need to repeatedly reheat the main solution. Another MDCr configuration submerges hollow fiber membranes in a tank, which could serve as both crystallizer and feed tank, and could reduce the heat loss from solution circulation [103] and transfer the crystallization location from the membrane surface to the bulk solution [104]. Increasing the feed flow rate increases the Reynolds number, thereby improving the mass and heat transfer coefficients, and thus the overall efficiency of the system [105]. There is an optimum flow rate to achieve the best economic benefit at the equilibrium point between energy consumption and flux [106]. Moreover, the interaction of different ions in the feed solution may influence the whole operation process (e.g., final crystal product morphology, product quality, and yield). Quist-Jensen et al. [107] found that, depending on the specific operating conditions, lithium chloride (LiCl) crystals could be obtained in cubic or orthorhombic polymorphic structures [107]. Salmón et al. [108] were able to obtain high-quality crystals without co-crystallization under the proper conditions.

Under reasonable MDCr operating conditions, it is possible to achieve a water–salt balance in the feed and output of the system, thereby achieving zero liquid discharge (ZLD) desalination [109]. Quist-Jensen et al. [110] integrated innovative membrane processes to achieve ZLD and recover magnesium and lithium salts in high qualities. Guo et al. [111] optimized a ZLD desalination plant using the AGMD process, and the energy consumption for the lab-scale equipment was as low as 1651.5 kJ per kilogram of water (H_2O). Lu et al. [112] established a mathematical model to build a ZLD system that integrates freeze desalination and MDCr (Fig. 16). This optimized hybrid system possessed a seawater treatment capacity of 72 kg·d^{-1}, and half of its energy consumption

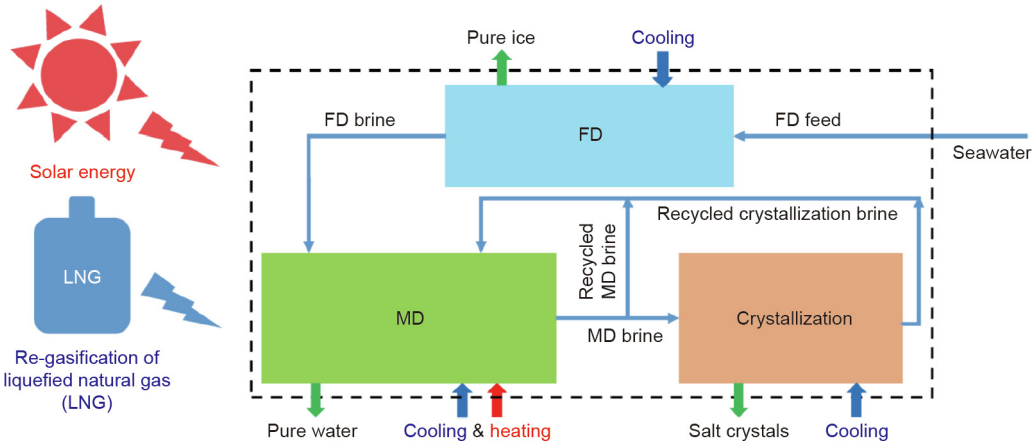

Fig. 16. Mechanism of the integrated MDCr and freeze desalination (FD) system with ZLD. Reproduced from Ref. [112] with permission of Elsevier Ltd., ©2019.

could be supported by a 50.5 m^2 solar panel, which provides a possible approach to realize ZLD using clean energy. As a process that could treat high-salinity wastewater while recovering pure water and high-quality salt products, MDCr could be used in the treatment of industrial wastewater. Kim et al. [113] reported that, for the treatment of shale gas production water, the recovery rate of freshwater and minerals with the MDCr process was up to 84% and 2.72 $kg \cdot m^{-2} \cdot d^{-1}$, respectively, with low energy consumption (28.2 $kW \cdot h \cdot m^{-3}$).

4.3. Control of membrane fouling and wetting in MCr

In the MDCr process it is desirable not only to promote crystal formation as much as possible to achieve higher yields, but also to avoid membrane fouling caused by crystallization in order to achieve continuous operation [114]. Ideally, the crystals detached from the membrane surface would be brought into the crystallizer via hydrodynamic transport, and crystal formation would be promoted by the nucleus to maintain the concentration balance [30,113,115]. In actuality, the deposition of crystals on the membrane surface significantly impacts the flux decline in the MDCr process [116,117]. Crystal products could be removed in a timely fashion to a certain extent using reasonable operating conditions [41,114]. Once fine crystals are generated on the membrane interface, it is difficult to reduce the membrane fouling by washing with pure water [118] and air backwashing. Thus, avoiding membrane fouling in the initial period, which is highly influenced by the solution system, is a key issue [119].

In some studies on seawater desalination via MCr, the main cause of flux decline is the deposition of calcium-based pollutants on the membrane interface [37,120]. As the calcium-based pollutants have low solubility, even if the solution does not reach saturation, adhesion of the micronuclei (or cluster) would cause crystal growth on the membrane surface, which greatly shortens the operation duration [121]. The main solution to this problem is adding various precipitants to reduce the concentration of calcium and magnesium ions. Drioli et al. [122] achieved reactive precipitations by adding $NaHCO_3/Na_2CO_3$ aqueous solutions of a certain concentration (1:1 Ca^{2+}/CO_3^{2-} molar ratio). Creusen et al. [123] added calcium carbonate ($CaCO_3$) crystals to the bulk solution to promote crystallization and prevent flux decline. Quist-Jensen et al. [110] found that 98% of Ca^{2+} ions could be precipitated when Na_2CO_3 was added at a 1:1.05 Ca^{2+}/CO_3^{2-} molar ratio. Membrane fouling also promotes the occurrence of membrane wetting [124,125]. Gryta [94] studied the mechanism of membrane wetting and the operating conditions that can produce membrane wetting via mathematical methods. Furthermore, it is easy for organic matter in the bulk solution to cause membrane wetting [126]. Thus, in practical applications, it is necessary to reduce organic matter via a pretreatment process [127]. Essentially, similarly to other membrane-based separation processes, the long-term operation of MCr will urgently require a new combined chemical and physical antifouling technology.

5. Conclusions and perspectives

With its expanding theoretical understanding and practical applications, MCr has become a frontier of the intersection of process engineering and product engineering, which is far beyond where its research initially started. Previous and ongoing studies have demonstrated the emerging attraction and feasibility of MCr technology for such applications as comprehensive wastewater treatment, desalination, enhanced micromixing, accurate nucleation control, and hybrid continuous crystallization intensification. Thus, all the recent research has illustrated that MCr-utilized membranes, process intensification mechanisms, and process control applications can inspire both crystallization engineering and membrane engineering. MCr may also lead to innovative development and improvements in high-level solid chemical manufacture.

The field of membrane crystallization could benefit from future efforts in the following areas:

(1) Miniaturization of the membrane module for advanced nucleation and growth control technology.

(2) Continuous stable process models for MCr process design with multiple targets, such as energy efficiency, crystal size distribution, crystal morphology, and crystal shape selectivity.

(3) Improved membrane and control technology that can convert membrane scaling and particle deposition to particle autodetachment.

(4) Development of membrane-assisted reactive crystallization for nanoparticle, pharmaceutical, and biological crystal manufacture.

Acknowledgements

We acknowledge the financial contributions from the National Natural Science Foundation of China (21978037, 21676043, 21527812, and U1663223), the Ministry of Science and Technology of the People's Republic of China innovation team in key area (2016RA4053), and Fundamental Research Funds for the Central Universities (DUT19TD33).

Compliance with ethics guidelines

Xiaobin Jiang, Yushan Shao, Lei Sheng, Peiyu Li, and Gaohong He declare that they have no conflict of interest or financial conflicts to disclose.

References

[1] Kiani H, Sun DW. Water crystallization and its importance to freezing of foods: a review. Trends Food Sci Technol 2011;22(8):407–26.
[2] Sha Z, Yin Q, Chen J. Industrial crystallization: trends and challenges. Chem Eng Technol 2013;36(8):1286.
[3] Morris G, Power G, Ferguson S, Barrett M, Hou G, Glennon B. Estimation of nucleation and growth kinetics of benzoic acid by population balance modeling of a continuous cooling mixed suspension, mixed product removal crystallizer. Org Process Res Dev 2015;19(12):1891–902.
[4] Bhangu SK, Ashokkumar M, Lee J. Ultrasound assisted crystallization of paracetamol: crystal size distribution and polymorph control. Cryst Growth Des 2016;16(4):1934–41.
[5] Tao F, Han Q, Liu K, Yang P. Tuning crystallization pathways through the mesoscale assembly of biomacromolecular nanocrystals. Angew Chem Int Ed Engl 2017;56(43):13440–4.
[6] Zhang D, Xu S, Du S, Wang J, Gong J. Progress of pharmaceutical continuous crystallization. Engineering 2017;3(3):354–64.
[7] Lakerveld R, Verzijden NG, Kramer H, Jansens P, Grievink J. Application of ultrasound for start-up of evaporative batch crystallization of ammonium sulfate in a 75-L crystallizer. AIChE J 2011;57(12):3367–77.
[8] Nguyen TNP, Kim KJ. Transformation of hemipentahydrate to monohydrate of risedronate monosodium by seed crystallization in solution. AIChE J 2011;57(12):3385–94.
[9] Soare A, Dijkink R, Pascual MR, Sun C, Cains PW, Lohse D, et al. Crystal nucleation by laser-induced cavitation. Cryst Growth Des 2011;11(6):2311–6.
[10] Narducci O, Jones AG. Seeding *in situ* the cooling crystallization of adipic acid using ultrasound. Cryst Growth Des 2012;12(4):1727–35.
[11] Chandrapala J, Oliver CM, Kentish S, Ashokkumar M. Use of power ultrasound to improve extraction and modify phase transitions in food processing. Food Rev Int 2013;29(1):67–91.
[12] Susanto H. Towards practical implementations of membrane distillation. Chem Eng Process 2011;50(2):139–50.
[13] Zuo J, Chung TS. *In-situ* cross-linked PVDF membranes with enhanced mechanical durability for vacuum membrane distillation. AIChE J 2016;62(11):4013–22.
[14] Adrjanowicz K, Koperwas K, Paluch M. Isobaric cooling or isothermal compression? Unveiling the effect of path dependence on crystallization. Cryst Growth Des 2017;17(6):2950–4.
[15] Lu D, Li P, Xiao W, He G, Jiang X. Simultaneous recovery and crystallization control of saline organic wastewater by membrane distillation crystallization. AIChE J 2017;63(6):2187–97.

[16] Alpatova A, Alsaadi AS, Alharthi M, Lee JG, Ghaffour N. Co-axial hollow fiber module for air gap membrane distillation. J Membr Sci 2019;578:172–82.
[17] Cheng C, Shao Z, Vollrath F. Silk fibroin-regulated crystallization of calcium carbonate. Adv Funct Mater 2008;18(15):2172–9.
[18] Zimmermann NER, Vorselaars B, Quigley D, Peters B. Nucleation of NaCl from aqueous solution: critical sizes, ion-attachment kinetics, and rates. J Am Chem Soc 2015;137(41):13352–61.
[19] Di Profio G, Salehi SM, Caliandro R, Guccione P, Nico G, Curcio E, et al. Bioinspired synthesis of $CaCO_3$ superstructures through a novel hydrogel composite membranes mineralization platform: a comprehensive view. Adv Mater 2016;28(4):610–6.
[20] Khayet M. Membranes and theoretical modeling of membrane distillation: a review. Adv Colloid Interface Sci 2011;164(1–2):56–88.
[21] Chen DY, Wang B, Sirkar KK. Hydrodynamic modeling of porous hollow fiber anti-solvent crystallizer for continuous production of drug crystals. J Membr Sci 2018;556:185–95.
[22] Jiang X, Lu D, Xiao W, Ruan X, Fang J, He G. Membrane assisted cooling crystallization: process model, nucleation, metastable zone, and crystal size distribution. AIChE J 2016;62(3):829–41.
[23] Zuo J, Chung TS. PVDF hollow fibers with novel sandwich structure and superior wetting resistance for vacuum membrane distillation. Desalination 2017;417:94–101.
[24] Luo L, Chang J, Chung TS. Cooling crystallization of sodium chloride via hollow fiber devices to convert waste concentrated brines to useful products. Ind Eng Chem Res 2017;56(36):10183–92.
[25] Jiang X, Tuo L, Lu D, Hou B, Chen W, He G. Progress in membrane distillation crystallization: process models, crystallization control and innovative applications. Front Chem Sci Eng 2017;11(4):647–62.
[26] Jiang X, Li G, Lu D, Xiao W, Ruan X, Li X, et al. Hybrid control mechanism of crystal morphology modification for ternary solution treatment via membrane assisted crystallization. Cryst Growth Des 2018;18(2):934–43.
[27] Zarkadas DM, Sirkar KK. Solid hollow fiber cooling crystallization. Ind Eng Chem Res 2004;43(22):7163–80.
[28] Iliuta I, Iliuta MC. Investigation of CO_2 removal by immobilized carbonic anhydrase enzyme in a hollow-fiber membrane bioreactor. AIChE J 2017;63(7):2996–3007.
[29] Tuo L, Ruan X, Xiao W, Li X, He G, Jiang X. A novel hollow fiber membrane-assisted antisolvent crystallization for enhanced mass transfer process control. AIChE J 2019;65(2):734–44.
[30] Jiang X, Lu D, Xiao W, Li G, Zhao R, Li X, et al. Interface-based crystal particle autoselection via membrane crystallization: from scaling to process control. AIChE J 2019;65(2):723–33.
[31] Schrimpf M, Esteban J, Rösler T, Vorholt AJ, Leitner W. Intensified reactors for gas–liquid–liquid multiphase catalysis: from chemistry to engineering. Chem Eng J 2019;372:917–39.
[32] Keil FJ. Process intensification. Rev Chem Eng 2018;34(2):135–200.
[33] Wang R, Li XG, Na J, Wu Y, Zhao RN, Yan YT, et al. Reversible reaction-assisted intensification process for separating ethanediol and 1,2-butanediol: competitive kinetics study and conceptual design. Sep Purif Technol 2020;237:116323.
[34] Sparenberg MC, Ruiz Salmón I, Luis P. Economic evaluation of salt recovery from wastewater via membrane distillation–crystallization. Sep Purif Technol 2020;235:116075.
[35] Ruiz Salmón I, Simon K, Clérin C, Luis P. Salt recovery from wastewater using membrane distillation–crystallization. Cryst Growth Des 2018;18(12):7275–85.
[36] Choi Y, Naidu G, Nghiem LD, Lee S, Vigneswaran S. Membrane distillation crystallization for brine mining and zero liquid discharge: opportunities, challenges, and recent progress. Environ Sci Water Res Technol 2019;5(7):1202–21.
[37] Drioli E, Di Profio G, Curcio E. Progress in membrane crystallization. Curr Opin Chem Eng 2012;1(2):178–82.
[38] Das P, Dutta S, Singh KKK, Maity S. Energy saving integrated membrane crystallization: a sustainable technology solution. Sep Purif Technol 2019;228:115722.
[39] Polino M, Portugal CAM, Di Profio G, Coelhoso IM, Crespo JG. Protein crystallization by membrane-assisted technology. Cryst Growth Des 2019;19(8):4871–83.
[40] Ismail AF, Goh PS, Sanip SM, Aziz M. Transport and separation properties of carbon nanotube-mixed matrix membrane. Sep Purif Technol 2009;70(1):12–26.
[41] Edwie F, Chung TS. Development of hollow fiber membranes for water and salt recovery from highly concentrated brine via direct contact membrane distillation and crystallization. J Membr Sci 2012;421–422:111–23.
[42] Moore DT, Sai H, Tan KW, Smilgies DM, Zhang W, Snaith HJ, et al. Crystallization kinetics of organic–inorganic trihalide perovskites and the role of the lead anion in crystal growth. J Am Chem Soc 2015;137(6):2350–8.
[43] Bouchrit R, Boubakri A, Mosbahi T, Hafiane A, Bouguecha SAT. Membrane crystallization for mineral recovery from saline solution: study case Na_2SO_4 crystals. Desalination 2017;412:1–12.
[44] Chen D, Singh D, Sirkar KK, Pfeffer R. Continuous synthesis of polymer-coated drug particles by porous hollow fiber membrane-based antisolvent crystallization. Langmuir 2015;31(1):432–41.
[45] Chen D, Singh D, Sirkar KK, Pfeffer R. Porous hollow fiber membrane-based continuous technique of polymer coating on submicron and nanoparticles via antisolvent crystallization. Ind Eng Chem Res 2015;54(19):5237–45.
[46] Choi Y, Naidu G, Lee S, Vigneswaran S. Recovery of sodium sulfate from seawater brine using fractional submerged membrane distillation crystallizer. Chemosphere 2020;238:124641.
[47] Liu F, Hashim NA, Liu Y, Abed MRM, Li K. Progress in the production and modification of PVDF membranes. J Membr Sci 2011;375(1–2):1–27.
[48] Feng CY, Khulbe KC, Matsuura T, Ismail AF. Recent progress in polymeric hollow-fibre membrane preparation, characterization and applications. Sep Purif Technol 2013;113:43–71.
[49] Ruan X, He G, Li B, Xiao J, Dai Y. Cleaner recovery of tetrafluoroethylene by coupling residue-recycled polyimide membrane unit to distillation. Sep Purif Technol 2014;124:89–98.
[50] Rajabzadeh S, Maruyama T, Sotani T, Matsuyama H. Preparation of PVDF hollow fiber membrane from a ternary polymer/solvent/nonsolvent system via thermally induced phase separation (TIPS) method. Sep Purif Technol 2008;63(2):415–23.
[51] Shang M, Matsuyama H, Teramoto M, Lloyd DR, Kubota N. Preparation and membrane performance of poly(ethylene-*co*-vinyl alcohol) hollow fiber membrane via thermally induced phase separation. Polymer 2003;44(24):7441–7.
[52] Anisi F, Thomas KM, Kramer HJM. Membrane-assisted crystallization: membrane characterization, modelling and experiments. Chem Eng Sci 2017;158:277–86.
[53] Choi Y, Naidu G, Jeong S, Lee S, Vigneswaran S. Fractional-submerged membrane distillation crystallizer (F-SMDC) for treatment of high salinity solution. Desalination 2018;440:59–67.
[54] Kaufhold D, Kopf F, Wolff C, Beutel S, Hilterhaus L, Hoffmann M, et al. Generation of Dean vortices and enhancement of oxygen transfer rates in membrane contactors for different hollow fiber geometries. J Membr Sci 2012;423–424:342–7.
[55] Criscuoli A, Bafaro P, Drioli E. Vacuum membrane distillation for purifying waters containing arsenic. Desalination 2013;323:17–21.
[56] Di Profio G, Tucci S, Curcio E, Drioli E. Selective glycine polymorph crystallization by using microporous membranes. Cryst Growth Des 2007;7(3):526–30.
[57] Di Profio G, Curcio E, Drioli E. Trypsin crystallization by membrane-based techniques. J Struct Biol 2005;150(1):41–9.
[58] Di Profio G, Polino M, Nicoletta FP, Belviso BD, Caliandro R, Fontananova E, et al. Tailored hydrogel membranes for efficient protein crystallization. Adv Funct Mater 2014;24(11):1582–90.
[59] Wang L, He G, Ruan X, Zhang D, Xiao W, Li X, et al. Tailored robust hydrogel composite membranes for continuous protein crystallization with ultrahigh morphology selectivity. ACS Appl Mater Interfaces 2018;10:26653–61.
[60] Yao C, Zhao Y, Ye C, Dang M, Dong Z, Chen G. Characteristics of slug flow with inertial effects in a rectangular microchannel. Chem Eng Sci 2013;95:246–56.
[61] Ghanem A, Lemenand T, Della Valle D, Peerhossaini H. Static mixers: mechanisms, applications, and characterization methods—a review. Chem Eng Res Des 2014;92(2):205–28.
[62] Liang Y, Chu G, Wang J, Huang Y, Chen J, Sun B, et al. Controllable preparation of nano-$CaCO_3$ in a microporous tube-in-tube microchannel reactor. Chem Eng Process 2014;79:34–9.
[63] Wang J, Li F, Lakerveld R. Process intensification for pharmaceutical crystallization. Chem Eng Process 2018;127:111–26.
[64] Belca LM, Ručigaj A, Teslič D, Krajnc M. The use of ultrasound in the crystallization process of an active pharmaceutical ingredient. Ultrason Sonochem 2019;58:104642.
[65] Guo Z, Han W, Zhao W, Li L, Wang B, Xiao Y, et al. The effect of microwave on the crystallization process of magnesium carbonate from aqueous solutions. Powder Technol 2018;328:358–66.
[66] Koizumi H, Tomita Y, Uda S, Fujiwara K, Nozawa J. Nucleation rate enhancement of porcine insulin by application of an external AC electric field. J Cryst Growth 2012;352(1):155–7.
[67] Li Y, Wang S, Sun B, Arowo M, Zou H, Chen J, et al. Visual study of liquid flow in a rotor-stator reactor. Chem Eng Sci 2015;134:521–30.
[68] Zhang F, Liu T, Wang XZ, Liu J, Jiang X. Comparative study on ATR–FTIR calibration models for monitoring solution concentration in cooling crystallization. J Cryst Growth 2017;459:50–5.
[69] Drioli E, Stankiewicz AI, Macedonio F. Membrane engineering in process intensification—an overview. J Membr Sci 2011;380(1–2):1–8.
[70] Van Gerven T, Stankiewicz A. Structure, energy, synergy, times—the fundamentals of process intensification. Ind Eng Chem Res 2009;48(5):2465–74.
[71] Ponce-Ortega JM, Al-Thubaiti MM, El-Halwagi MM. Process intensification: new understanding and systematic approach. Chem Eng Process 2012;53:63–75.
[72] Sinibaldi G, Romano GP. Flow configurations in a Y splitting-junction microchannel. Fluids 2017;2(2):18.
[73] Yao C, Liu Y, Xu C, Zhao S, Chen G. Formation of liquid–liquid slug flow in a microfluidic T-junction: effects of fluid properties and leakage flow. AIChE J 2018;64(1):346–57.
[74] Zhang F, Marre S, Erriguible A. Mixing intensification under turbulent conditions in a high pressure microreactor. Chem Eng J 2020;382:122859.
[75] Macchi A, Plouffe P, Patience GS, Roberge DM. Experimental methods in chemical engineering: micro-reactors. Can J Chem Eng 2019;97(10):2578–87.
[76] Falk L, Commenge JM. Performance comparison of micromixers. Chem Eng Sci 2010;65(1):405–11.

[77] Hosseini SM, Razzaghi K, Shahraki F. Design and characterization of a low-pressure-drop static mixer. AIChE J 2019;65(3):1126–33.
[78] Ye W, Lin J, Madsen HT, Søgaard EG, Hélix-Nielsen C, Luis P, et al. Enhanced performance of a biomimetic membrane for Na_2CO_3 crystallization in the scenario of CO_2 capture. J Membr Sci 2016;498:75–85.
[79] Lu Y, Zhang T, Liu Y, Luo G. Preparation of $FePO_4$ nano-particles by coupling fast precipitation in membrane dispersion microcontactor and hydrothermal treatment. Chem Eng J 2012;210:18–25.
[80] Chen GG, Luo GS, Xu JH, Wang JD. Membrane dispersion precipitation method to prepare nanopartials. Powder Technol 2004;139(2):180–5.
[81] Yang L, Guo M, Zhang F, Jing Y, Wang Y, Luo G. Controllable preparation of γ-alumina nanoparticles with bimodal pore size distribution in membrane dispersion microreactor. Particuology 2018;41:1–10.
[82] Wang Y, Zhang C, Bi S, Luo G. Preparation of ZnO nanoparticles using the direct precipitation method in a membrane dispersion micro-structured reactor. Powder Technol 2010;202(1–3):130–6.
[83] Yao H, Wang Y, Luo G. A size-controllable precipitation method to prepare CeO_2 nanoparticles in a membrane dispersion microreactor. Ind Eng Chem Res 2017;56(17):4993–9.
[84] Di Profio G, Stabile C, Caridi A, Curcio E, Drioli E. Antisolvent membrane crystallization of pharmaceutical compounds. J Pharm Sci 2009;98(12):4902–13.
[85] Zarkadas DM, Sirkar KK. Antisolvent crystallization in porous hollow fiber devices. Chem Eng Sci 2006;61(15):5030–48.
[86] Fern JCW, Ohsaki S, Watano S, Pfeffer R. Continuous synthesis of nano-drug particles by antisolvent crystallization using a porous hollow-fiber membrane module. Int J Pharm 2018;543(1–2):139–50.
[87] Zhou X, Zhu X, Wang B, Li J, Liu Q, Gao X, et al. Continuous production of drug nanocrystals by porous hollow fiber-based anti-solvent crystallization. J Membr Sci 2018;564:682–90.
[88] Sanmartino JA, Khayet M, García-Payo MC, El Bakouri H, Riaza A. Desalination and concentration of saline aqueous solutions up to supersaturation by air gap membrane distillation and crystallization fouling. Desalination 2016;393:39–51.
[89] Warsinger DM, Swaminathan J, Guillen-Burrieza E, Arafat HA, Lienhard JHV. Scaling and fouling in membrane distillation for desalination applications: a review. Desalination 2015;356:294–313.
[90] Macedonio F, Curcio E, Drioli E. Integrated membrane systems for seawater desalination: energetic and exergetic analysis, economic evaluation, experimental study. Desalination 2007;203(1–3):260–76.
[91] Ji X, Curcio E, Al Obaidani S, Di Profio G, Fontananova E, Drioli E. Membrane distillation–crystallization of seawater reverse osmosis brines. Sep Purif Technol 2010;71(1):76–82.
[92] Ali A, Quist-Jensen CA, Drioli E, Macedonio F. Evaluation of integrated microfiltration and membrane distillation/crystallization processes for produced water treatment. Desalination 2018;434:161–8.
[93] Wu Y, Kong Y, Liu J, Zhang J, Xu J. An experimental study on membrane distillation–crystallization for treating waste water in taurine production. Desalination 1991;80(2–3):235–42.
[94] Gryta M. Concentration of NaCl solution by membrane distillation integrated with crystallization. Sep Sci Technol 2002;37(15):3535–58.
[95] Pramanik BK, Thangavadivel K, Shu L, Jegatheesan V. A critical review of membrane crystallization for the purification of water and recovery of minerals. Rev Environ Sci Biotechnol 2016;15(3):411–39.
[96] Shirazi MMA, Kargari A. Concentrating of sugar syrup in bioethanol production using sweeping gas membrane distillation. Membranes 2019;9(5):59.
[97] Lawson KW, Lloyd DR. Membrane distillation. J Membr Sci 1997;124(1):1–25.
[98] Quist-Jensen CA, Sørensen JM, Svenstrup A, Scarpa L, Carlsen TS, Jensen HC, et al. Membrane crystallization for phosphorus recovery and ammonia stripping from reject water from sludge dewatering process. Desalination 2018;440:156–60.
[99] Vane LM. Review: water recovery from brines and salt-saturated solutions: operability and thermodynamic efficiency considerations for desalination technologies. J Chem Technol Biotechnol 2017;92(10):2506–18.
[100] Yu W, Graham N, Yang Y, Zhou Z, Campos LC. Effect of sludge retention on UF membrane fouling: the significance of sludge crystallization and EPS increase. Water Res 2015;83:319–28.
[101] Francis L, Ghaffour N, Al-Saadi AS, Amy G. Performance of different hollow fiber membranes for seawater desalination using membrane distillation. Desalin Water Treat 2015;55(10):2786–91.
[102] Meng S, Ye Y, Mansouri J, Chen V. Crystallization behavior of salts during membrane distillation with hydrophobic and superhydrophobic capillary membranes. J Membr Sci 2015;473:165–76.
[103] Julian H, Meng S, Li H, Ye Y, Chen V. Effect of operation parameters on the mass transfer and fouling in submerged vacuum membrane distillation crystallization (VMDC) for inland brine water treatment. J Membr Sci 2016;520:679–92.
[104] Zou T, Kang G, Zhou M, Li M, Cao Y. Submerged vacuum membrane distillation crystallization (S-VMDC) with turbulent intensification for the concentration of NaCl solution. Sep Purif Technol 2019;211:151–61.
[105] Shirazi MMA, Kargari A, Ismail AF, Matsuura T. Computational fluid dynamic (CFD) opportunities applied to the membrane distillation process: state-of-the-art and perspectives. Desalination 2016;377:73–90.
[106] Li W, Van der Bruggen B, Luis P. Integration of reverse osmosis and membrane crystallization for sodium sulphate recovery. Chem Eng Process 2014;85:57–68.
[107] Quist-Jensen CA, Ali A, Mondal S, Macedonio F, Drioli E. A study of membrane distillation and crystallization for lithium recovery from high-concentrated aqueous solutions. J Membr Sci 2016;505:167–73.
[108] Salmón IR, Simon K, Clérin C, Luis P. Salt recovery from wastewater using membrane distillation–crystallization. Cryst Growth Des 2018;18(12):7275–85.
[109] Guan G, Wang R, Wicaksana F, Yang X, Fane AG. Analysis of membrane distillation crystallization system for high salinity brine treatment with zero discharge using Aspen flowsheet simulation. Ind Eng Chem Res 2012;51(41):13405–13.
[110] Quist-Jensen CA, Macedonio F, Drioli E. Membrane crystallization for salts recovery from brine—an experimental and theoretical analysis. Desalin Water Treat 2016;57(16):7593–603.
[111] Guo H, Ali HM, Hassanzadeh A. Simulation study of flat-sheet air gap membrane distillation modules coupled with an evaporative crystallizer for zero liquid discharge water desalination. Appl Therm Eng 2016;108:486–501.
[112] Lu KJ, Cheng ZL, Chang J, Luo L, Chung TS. Design of zero liquid discharge desalination (ZLDD) systems consisting of freeze desalination, membrane distillation, and crystallization powered by green energies. Desalination 2019;458:66–75.
[113] Kim J, Kim J, Hong S. Recovery of water and minerals from shale gas produced water by membrane distillation crystallization. Water Res 2018;129:447–59.
[114] Macedonio F, Drioli E. Hydrophobic membranes for salts recovery from desalination plants. Desalin Water Treat 2010;18(1–3):224–34.
[115] Shin Y, Sohn J. Mechanisms for scale formation in simultaneous membrane distillation crystallization: effect of flow rate. J Ind Eng Chem 2016;35:318–24.
[116] Macedonio F, Quist-Jensen CA, Al-Harbi O, Alromaih H, Al-Jlil SA, Al Shabouna F, et al. Thermodynamic modeling of brine and its use in membrane crystallizer. Desalination 2013;323:83–92.
[117] Curcio E, Drioli E. Membrane distillation and related operations—a review. Sep Purif Rev 2005;34(1):35–86.
[118] Chen G, Lu Y, Krantz WB, Wang R, Fane AG. Optimization of operating conditions for a continuous membrane distillation crystallization process with zero salty water discharge. J Membr Sci 2014;450:1–11.
[119] Julian H, Ye Y, Li H, Chen V. Scaling mitigation in submerged vacuum membrane distillation and crystallization (VMDC) with periodic air-backwash. J Membr Sci 2018;547:19–33.
[120] Choi Y, Naidu G, Jeong S, Lee S, Vigneswaran S. Effect of chemical and physical factors on the crystallization of calcium sulfate in seawater reverse osmosis brine. Desalination 2018;426:78–87.
[121] Choi Y, Naidu G, Jeong S, Vigneswaran S, Lee S, Wang R, et al. Experimental comparison of submerged membrane distillation configurations for concentrated brine treatment. Desalination 2017;420:54–62.
[122] Drioli E, Curcio E, Criscuoli A, Di Profio G. Integrated system for recovery of $CaCO_3$, NaCl and $MgSO_4{\cdot}7H_2O$ from nanofiltration retentate. J Membr Sci 2004;239(1):27–38.
[123] Creusen R, van Medevoort J, Roelands M, van Renesse van Duivenbode A, Hanemaaijer JH, van Leerdam R. Integrated membrane distillation–crystallization: process design and cost estimations for seawater treatment and fluxes of single salt solutions. Desalination 2013;323:8–16.
[124] Naidu G, Jeong S, Vigneswaran S, Hwang TM, Choi YJ, Kim SH. A review on fouling of membrane distillation. Desalin Water Treat 2016;57(22):10052–76.
[125] Gryta M, Barancewicz M. Influence of morphology of PVDF capillary membranes on the performance of direct contact membrane distillation. J Membr Sci 2010;358(1–2):158–67.
[126] Naidu G, Jeong S, Choi Y, Vigneswaran S. Membrane distillation for wastewater reverse osmosis concentrate treatment with water reuse potential. J Membr Sci 2017;524:565–75.
[127] Kim J, Kwon H, Lee S, Lee S, Hong S. Membrane distillation (MD) integrated with crystallization (MDC) for shale gas produced water (SGPW) treatment. Desalination 2017;403:172–8.